AIAA 2002-1036

Reduction of Wake-Stator Interaction Noise Using Passive Porosity

Ana F. Tinetti, Jeffrey J. Kelly
Virginia Polytechnic Institute and State University / VCES
Hampton, VA

Russell H. Thomas, Steven X. S. Bauer
NASA Langley Research Center
Hampton, VA

40th AIAA Aerospace Sciences Meeting and Exhibit
14-17 January 2002 / Reno, NV

REDUCTION OF WAKE-STATOR INTERACTION NOISE USING PASSIVE POROSITY

Ana F. Tinetti[*], Jeffrey J. Kelly[†]
Virginia Polytechnic Institute and State University / VCES
Hampton, VA, 23666

Russell H. Thomas[§], Steven X. S. Bauer[‡]
NASA Langley Research Center
Hampton, VA, 23681

Abstract

The present study was conducted to assess the potential of Passive Porosity Technology as a mechanism to reduce interaction noise in turbomachinery by reducing the fluctuating forces acting on the vane surfaces. To do so, a typical fan stator airfoil was subjected to the effects of a transversely moving wake; time histories of the primitive aerodynamic variables, obtained from Computational Fluid Dynamics (CFD) solutions, were then input into an acoustic prediction code. This procedure was performed on the solid airfoil to obtain a baseline, and on a series of porous configurations in order to isolate those that yield maximum noise reductions without compromising the aerodynamic performance of the stator. It was found that communication between regions of high pressure differential - made possible by the use of passive porosity - is necessary to significantly alter the noise radiation pattern of the stator airfoil. In general, noise reductions were obtained for those configurations incorporating passive porosity in the region between $x/c \sim 0.15$ on the suction side of the airfoil and $x/c \sim 0.20$ on the pressure side. Reductions in overall radiated noise of approximately 1.0 dB were obtained. The noise benefit increased to about 2.5 dB when the effects of loading noise alone were considered.

Nomenclature

M   Local Mach number
V_n Local flow velocity normal to porous surface
a   Speed of sound
c   Stator chord
c_l Stator airfoil lift coefficient
c_d Stator airfoil drag coefficient
l Incoming gust wavelength
p   Local flow static pressure
s   Solidity
u, w   Cartesian velocities in x and z directions
x, z   Cartesian coordinates
γ Ratio of specific heats, $\gamma = 1.4$ for air
ρ Local flow density
ω Reduced frequency parameter, $\omega = \frac{\pi c}{l}$; also angular frequency

Subscripts

0   Start of wake traverse, t = 0.0 seconds
1   Upstream of porous surface
2   Minimum area of flow through porous surface
3   Fully mixed flow region, downstream of surface
t   Stagnation condition
w   Wake effects
∞ Freestream conditions

Introduction

For typical high-bypass turbofan engines, fan noise, radiated forward through the inlet and aft through the fan exhaust duct, is the dominant source of noise during approach and takeoff conditions. Basically, fan noise is generated at the rotating blades and stationary vanes and struts, and can be of three types[1]: discrete tones, broadband, and multiple tones. During approach conditions, the local flow is subsonic and discrete tones are superimposed on a broadband component. During takeoff, supersonic speeds may be reached in the rotor blade tip region; if so, then all multiples of shaft frequency appear. Discrete tones occur at the blade passage frequency (BPF) and its harmonics, and are greatly influenced by the flow conditions over the rotor blades and by rotor-stator interactions: as a rotor wake passes by and impinges on a stator, the effective angle of attack and the velocity of the relative flow change, producing transient fluctuations in the pressure field acting on the stator vane surfaces. This unsteady pressure field gener-

---

[*]   Graduate Research Assistant, Mechanical Engineering Department, Senior Member AIAA.

[†]   Research Associate Professor, Mechanical Engineering Department, Senior Member AIAA. Currently with Northrop-Grumman.

[§]   Aerospace Engineer, Aeroacoustics Branch, Senior Member AIAA.

[‡]   Senior Research Engineer, Configuration Aerodynamics Branch, Associate Fellow AIAA.

ates a lift force that fluctuates with a frequency equal to the blade passing rate, and that is distributed over the stator vane surface. The fluctuating force gives rise to a dipole-type noise source. Generally, there is a sequential phasing of the wake interaction around the vane assembly caused by the different number of rotors and stators in the fan stage. This phasing forms a periodic pattern that sweeps circumferentially around the vane array and can easily propagate in a spiral fashion along and out the fan duct.

Fan noise reduction can be achieved either by designing for it at the source or by incorporating acoustic treatment to absorb the noise produced by the source. Approaches to reduce noise at the source are based on the fact that any of the significant noise generating mechanisms is related to unsteady, periodic forces acting on the rotor blade and stator vane surfaces, and caused by gust-type disturbances. These unsteady forces give rise to acoustic perturbations that propagate through the fan duct and radiate as noise. The amplitude of the noise generated from this source is directly proportional to the magnitude of the fluctuating lift force. Thus, any reduction in this fluctuating force would result in a reduction in noise.

From the noise reduction stand point, the aerodynamic parameters associated with rotor-stator interaction can be grouped into those that (1) would reduce the amplitude of the wakes shed by the rotors, and (2) would reduce the response of the stators to impinging wakes. The amplitude of the wakes impinging on the stators can be reduced by increasing the spacing between the rotors and stators[2,3], which allows the wakes generated by the rotors to decay and dissipate before impinging on the stators; and by reducing rotor blade drag[2,4], which is directly proportional to the maximum velocity defect of the wakes. It has been determined[5] that the response of a stator to incoming wakes is inversely proportional to the reduced frequency parameter ω (= $\pi c/l$, where c is the stator chord and l is the wavelength of the incoming gust). Increments in ω can be achieved by increasing the stator chord, which has the additional benefit of reducing the number of noise sources in a given design by reducing the number of stator vanes; and by reducing the gust wavelength[2]. The latter approach involves increasing the gust frequency, which can be achieved by increasing the number of wakes (i.e., the number of rotor blades).

Other methods have been suggested as well for the reduction of transient forces produced by wake interactions. For example, the use of staggered blades around the rotor and stator discs to impair wake periodicity[6]; the

slanting of one row of blades relative to the other to slightly reduce system efficiency[7], this reduction being caused by the inability to maintain an optimum blade load distribution; and the application of active control techniques to the stator in order to counter its unsteady response[8].

The methods currently available for reducing the components of fan noise at their sources are diverse. The potential noise gains that may result from the implementation of any of these methods have to be balanced against the associated increments in engine weight and/or decrements in performance. Although most of the approaches mentioned thus far are viable considerations in the design of new engines, their applicability to already existing power plants necessarily involves major efficiency and economic trade-offs. As an alternative, passive porosity[9] is a weight-neutral technology that can be easily incorporated into new engine designs and is highly suited for retrofitting existing ones.

Passive porosity redistributes pressure on the outer surface of a configuration by establishing communication between regions of high and low pressure through a plenum chamber located underneath the porous surface. This pressure redistribution, which is associated with a minute transfer of mass into and out of the plenum, changes the effective aerodynamic shape of the outer surface. This technology can be used to reduce wake velocity defects and stator response by reducing rotor drag and fluctuating stator lift, respectively. The potential noise reduction associated with the latter application of passive porosity is the subject of the present paper.

Computational Approach

In order to assess the feasibility of passive porosity as a viable mechanism to reduce wake-stator interaction noise, the porous surface model described in references 10 and 11 was implemented into a CFD code. Time histories of the primitive aerodynamic variables (ρ, u, v, p) were obtained for a typical stator vane airfoil subjected to the effects of a transversely moving wake, and then input into a noise prediction code. The process was performed on a solid airfoil to obtain a baseline, and on a series of porous airfoil configurations. The flow field around the wake-stator system was calculated using CFL3D[12]. Details about the aerodynamic results which form the basis for the noise calculations are found in references 10 and 13. The acoustic characteristics associated with the different airfoil configurations were obtained using FWH2D[14].

Porous Surface Model

Conservation of mass and momentum laws for the steady, one-dimensional, isentropic (adiabatic and reversible) flow of a perfect gas are used to simulate the average effects associated with the flow of air through a perforated plate of solidity s. In the following equations, states 1, 2, and 3 correspond to locations upstream of the porous surface, minimum area at which the jets formed by the screen holes are fully contracted but essentially undiffused, and downstream of the surface, respectively (see Figure 1).
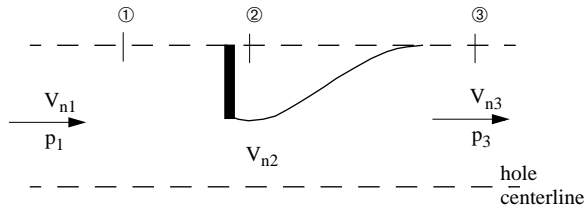

Figure 1.- Model of flow through a single screen hole.

The equations governing the flow of air through a screen or perforated plate are:

Conservation of mass:

$$(\rho V_n)_1 = (\rho V_n)_2 \phi(1-s) = (\rho V_n)_3 \qquad (1)$$

Conservation of momentum:

$$p_1(1 + \gamma M_1^2) = \qquad (2)$$
$$p_2[1 + \gamma M_2^2 \phi(1-s)] = p_3(1 + \gamma M_3^2)$$

Zero total pressure loss during jet formation:

$$p_{t1} = p_{t2} \qquad (3)$$

The empirical contraction coefficient ϕ is given by[15]

$$\phi = \phi_o + 0.185 s^{0.25}\left(\frac{p_{t2}}{p_2} - 1\right) \qquad (4)$$

where the incompressible component ϕ_0 is

$$\phi_o = \frac{0.04137}{1.0982 - (1-s)} + 0.57323 + 0.005786(1-s) \qquad (5)$$

The need to grid plenum chambers inside the airfoil, which are a required element of Passive Porosity Technology, was precluded by implementing the model into the flow solver as a homogeneous surface boundary condition, and by assuming that the chamber pressure is constant and known a priori. See references 10 and 11 for implementation details.

Flow Solver

CFL3D, developed at the NASA Langley Research Center (LaRC), solves the three-dimensional, time-dependent, thin-layer approximation to the Reynolds-Averaged Navier-Stokes (RANS) equations using a finite volume formulation in generalized coordinates. It uses upwind-biased spatial differencing for the inviscid terms, and central differences for the viscous and heat transfer terms. The code, which is second-order accurate in space, is advanced in time with an implicit three-factor approximate factorization (AF) scheme. Temporal subiterations with multigrid are used to recover time accuracy lost as a result of the AF approach during unsteady calculations. CFL3D includes several grid connection strategies, a vast array of zero-, one-, and two-equation turbulence models, numerous boundary conditions, and translating grid capabilities suitable for turbomachinery applications. The aerodynamic results used to calculate airfoil noise characteristics were obtained using the two-equation k-ω SST model of Menter[16].

Structured Grid

The computational setup chosen for the study consists of a single stator airfoil immersed in a subsonic flow field, subject to the effects of a transversely moving wake. The chosen section corresponds to the mid-span of one of the stator vanes composing the Pratt and Whitney Advanced Ducted Propeller high power fan model currently at NASA Langley[17]. The airfoil is oriented at an angle of attack that minimizes flow separation over its surface.

A two-dimensional, 9-zone grid was used to define the stator/wake system. The grid, which extends to 15 chords above and below the stator, was designed to minimize numerical dissipation as the wake traverses the stator flow field. The gust impinging on the stator is represented by a user-supplied wake having a 33% velocity defect at the plane of the stator leading edge. A translational speed of 78 c/s, corresponding to an angular velocity of 500 rpm, was chosen for the wake. Schematic representations of the grid, airfoil, and wake are given in Figure 2. Through the use of dynamic patched interfacing, the wake is displaced a distance of approximately 4 stator chords, from face k1 to face kmax of zone 5, by a downward translation of zones 5, 8 and 9. At the end of the specified traverse, the algorithm translates the moving blocks and their solution back to their original position. The entire wake traverse requires approximately 2230 time steps. The given wake translational speed, traversed distance, and free stream Mach number (0.166) guarantee that, at any given time, the

American Institute of Aeronautics and Astronautics

stator is subject to the passage of a single wake only. See references 10 and 13 for details on the wake-stator system.
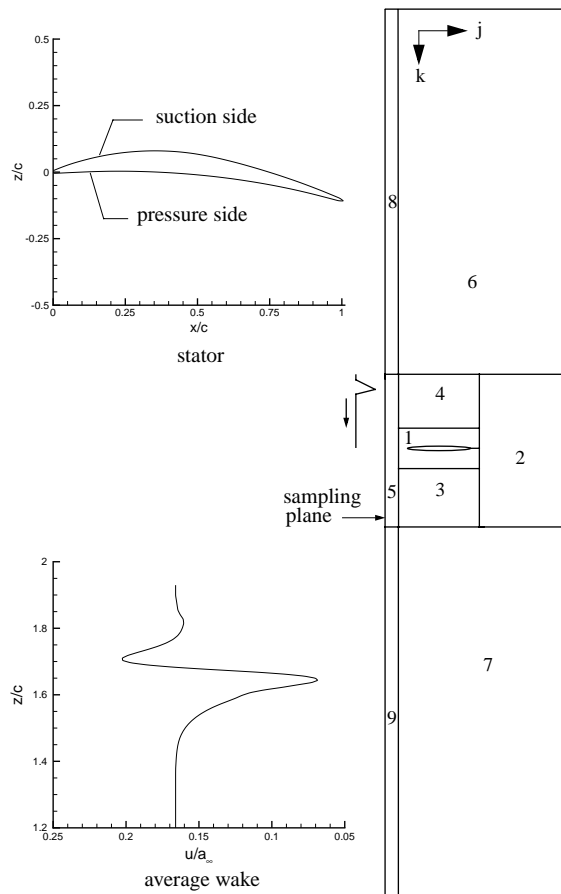

Figure 2.- Computational grid.

Noise Prediction Code

The advent of accurate, mature CFD codes and ever-increasing computer capabilities have promoted the use of integral techniques that can predict far field acoustic signals based solely on near-field input. The near-field input is usually in the form of highly resolved unsteady data obtained from converged CFD solutions. One of the most popular integral techniques is based on the Ffowcs-Williams and Hawkings (FW-H) equation, which is an exact rearrangement of the continuity and momentum equations into the form of an inhomogeneous wave equation having two surface source terms of monopole and dipole nature, and a volume source term of quadrupole nature. The monopole source is associated with thickness noise, which is determined by the geometry and kinematics of the body; the dipole source represents the noise generated by unsteady forces acting on the fluid as a result of the presence of the body, also

known as loading noise; and the quadrupole source accounts for non-linear effects such as convection, refraction, and viscous dissipation of sound by the mean flow, and scattering of sound by turbulence and variations in entropy[18]. The FW-H method has typically been applied by assuming that the integration surface is impenetrable and coincident with the physical body surface. However, this assumption is not necessary. In fact, the use of more general integration surfaces has resulted in successful predictions of the acoustic far field generated by bodies immersed in unsteady flows[19,20]. These predictions also demonstrated that a very important advantage of this new version of the FW-H method is that the quadrupole term need not be included if the integration surface contains the major sources of non-linear behavior.

FWH2D, also developed at NASA LaRC, is based on a two-dimensional formulation of the FW-H equation. The problem is transformed into the frequency domain in order to avoid time integration complications inherent to a two-dimensional solution of the FW-H equation. The function describing the general integration surface is given a uniform rectilinear motion time dependence prior to performing the required Fourier transformation into the frequency domain. Because any two-dimensional approach necessarily implies perfect correlation in the third dimension, the amplitude of the propagated sound is overpredicted using this method. However, since the focus of the present investigation is to determine the noise benefits that may result from the application of porosity to stator vane surfaces, any effects associated with this overprediction are obviated by considering changes in noise levels relative to a solid stator baseline.

Results and Discussion

The unsteady nature of the lift associated with a solid stator when subjected to wake convection is depicted in Figure 3. Note from the figure that the lift coefficient decreases as the wake approaches the stator, and then increases as the wake recedes. This behavior is directly related to the changes in pressure over the airfoil surface caused by the presence of the wake. As the wake moves past the stator, the local flow is subjected to transient fluctuations in velocity and turbulence intensity that affect the boundary layer, and thus, the surface pressure distribution. A maximum reduction in c_l of 29%, as measured from the reference value at the start of the wake traverse (t = 0.00 s), resulted from wake-stator interactions. This parameter is denoted as $(\Delta c_{l_w})_{max}$ in the present investigation. The reference c_l was obtained from a converged solution with the wake held stationary

at a distance of approximately 2 chords above the airfoil. No significant interaction between the wake and the stator was detected at this distance.
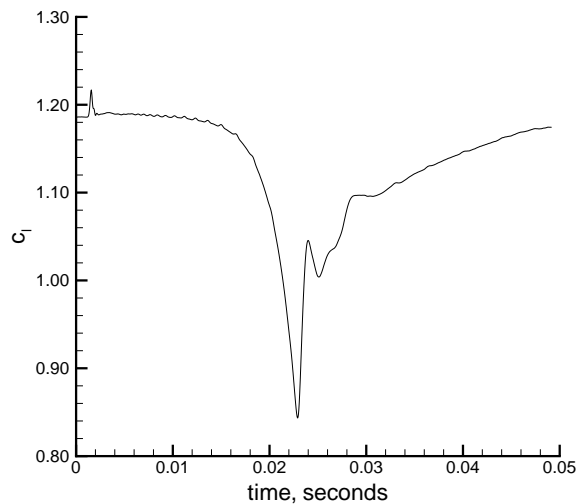

Figure 3.- Effect of wake passage on solid stator c_l, fine grid level. $M_\infty = 0.166$, $Re = 1.125 \times 10^6$, wake $\omega = 78$ c/s.

Porous Airfoil Parametric Study

The extent of the porous regions and their location on the stator surface depend, of course, on the intended application. For the reduction of unsteady interactions in turbomachinery environments, the overriding performance concern is the minimization of flow separation on the stator surfaces. Complementing this requirement, an acceptable porous configuration should not compromise airfoil performance, measured in terms of lift and drag coefficients at the start of the wake traverse ($t = 0.0$ s), $(c_l)_0$ and $(c_d)_0$, respectively.

A parametric study[10], involving approximately 50 different configurations, was performed in order to determine the effect of several porosity-related parameters on the aerodynamic and acoustic characteristics of a stator airfoil subjected to wake impingement. The parameters considered in the study were (1) the extent and location of the porous patches, ranging from full-chord porosity to small isolated regions near the leading edge (LE) and trailing edge (TE); (2) the configuration of the assumed plenum chamber - single or multiple, either connected or disconnected; (3) the surface porosity distribution, either constant or tapered with distance along the surface; and (4) the nominal porosity, varied approximately $\pm 10\%$ from a basis value of 22%[21].

It was found during the study that, for a single stator immersed in a subsonic flow field, communication between regions of high pressure differential - made possible by the use of passive porosity - tends to induce a time-dependent oscillatory pattern of small inflow-outflow regions near the stator LE, which is well established before wake effects come into play[10,13]. The oscillatory pattern starts at the LE, and travels downstream on both suction (leeward) and pressure (windward) sides of the airfoil. On the suction side, the pattern travels to the aft end of the patch and beyond. On the pressure side, the disturbances travel to approximately 50% of the patch extension. The amplitude of the oscillations on both sides of the airfoil seemed to be proportional to the extension of the porous patch on the pressure side.

Despite the presence of the oscillatory pattern, which would probably not arise if the airfoil were placed within a stator cascade and subject to flow conditions typical of turbomachinery environments, communication between regions of high pressure differential, especially near the LE, was found to be necessary in order to significantly alter the noise radiation pattern of the stator airfoil. Whether these changes result in noise abatement or enhancement depends primarily on the placement and extension of the porous patches, and on the configuration of the plenum chamber. In general, the porous airfoils that satisfied the study requirements - noise reduction with no flow separation and small relative changes in $(c_l)_0$ and $(c_d)_0$ - incorporated passive porosity in the LE region between $x/c \sim 0.15$ on the suction side and $x/c \sim 0.20$ on the pressure side. The passive porous surfaces in this region were either a single, continuous patch, or two non-adjacent patches with connected plenum chambers. The porous surface on the suction side was tapered elliptically from the nominal value to at most 10% to preclude the formation of a small recirculation area immediately downstream of the patch. Variations in nominal porosity were of secondary importance.

Most of the porous configurations tested were able to alleviate stator response to wake impingement, thus reducing the maximum change in c_l due to wake effects, $(\Delta c_{l_w})_{max}$. However, reductions in this parameter alone do not necessarily translate into overall decrements in radiated noise. In fact, the configurations yielding the largest noise reductions did not minimize $(\Delta c_{l_w})_{max}$. This trend has been observed previously[22], and it is most likely caused by the unsteadiness in the mean flow associated with wake convection.

In general, the better aerodynamic performers, i.e., those with smaller changes in $(c_l)_0$ and $(c_d)_0$, relative to solid stator values, were also the better acoustic performers. Some of these configurations will be used in the follow-

ing sections to discuss the effects of passive porosity on unsteady lift and radiated interaction noise.

Effect of Passive Porosity on Unsteady Lift

Some of the better aerodynamic/acoustic performers obtained from the parametric study are depicted in Figure 4. The first two configurations, e2 (denoted as A in reference 13) and f3e, have a suction side porosity distribution of 22% in the region $0 \leq x/c < 0.05$, then tapered elliptically from 22% to 10% in the region $0.05 \leq x/c \leq 0.10$. They also include an isolated 22% porosity patch in the region $0.95 \leq x/c \leq 1.0$ aimed at alleviating TE flow separation. It has been determined that this patch is not necessary, since, in general, viable configurations do not induce flow separation. However, it was included early in the study and kept for some of the configurations. Its effect is negligible. Configuration e2 has the same porosity distribution on both suction and pressure sides; configuration f3e is similar, except that the constant 22% porosity region on the pressure side extends to $x/c = 0.10$, and is then tapered to 10% from $x/c = 0.10$ to $x/c = 0.15$. The porous region is continuous on both sides, i.e., it is defined as a single patch.

Configuration n2 has two non-adjacent porous patches with communication between their respective plenum chambers. The main patch on the suction side has 22% porosity in the region $0.01 < x/c < 0.05$, with similar tapering as the others. The pressure side has a 22% porous patch on the region $0.15 < x/c < 0.25$. Thus, the vicinity of the stator LE remains solid.

(a) e2

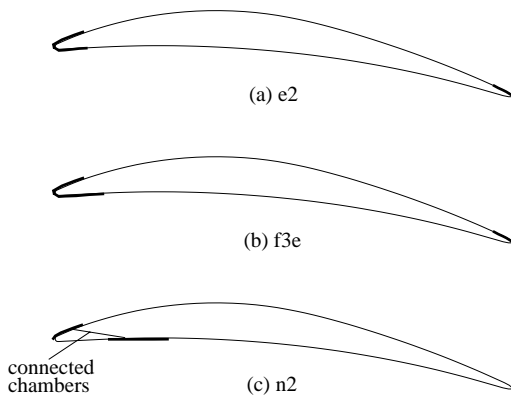(b) f3e

connected chambers

(c) n2

Figure 4.- Porous configurations for maximum reduction of wake-stator interaction noise.

Lift and drag coefficient time histories for the porous airfoil configurations are compared to the solid baseline in Figures 5 and 6, respectively. Although changes in the converged coefficients at the start of the traverse, $(c_l)_0$ and $(c_d)_0$, are inevitable because passive porosity alters

the effective aerodynamic shape of the airfoil, note from Figure 5 that reductions in $(c_l)_0$ (referenced to solid stator values) are small, being approximately 5.3%, 6%, and 4.9% for configurations e2, f3e, and n2, respectively. Corresponding increments in $(c_d)_0$ are 1%, 9%, and 11%. Decrements in $(\Delta c_{l_w})_{max}$ of 21%, 18%, and 19%, were obtained for configurations e2, f3e and n2, respectively.
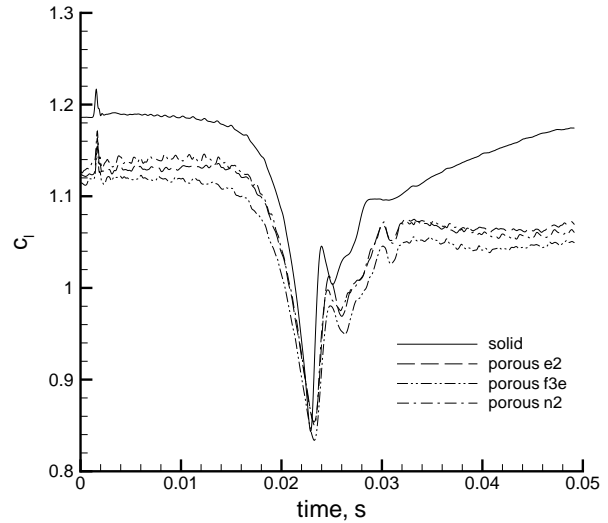

Figure 5.- Lift coefficient time histories for porous airfoil configurations, fine grid level. $M_\infty = 0.166$, $Re = 1.125 \times 10^6$, wake $\omega = 78$ c/s.
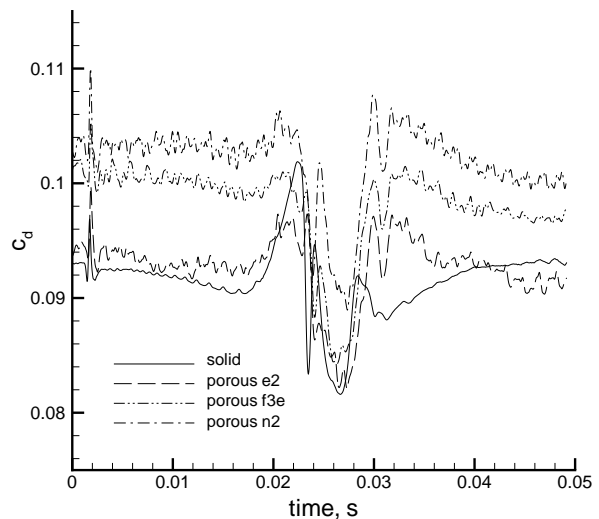

Figure 6.- Drag coefficient time histories for porous airfoil configurations, fine grid level. $M_\infty = 0.166$, $Re = 1.125 \times 10^6$, wake $\omega = 78$ c/s.

Effect of Passive Porosity on Interaction Noise

Time histories for the primitive aerodynamic variables corresponding to the time period shown in Figures 3, 5,

and 6 were input into FWH2D to obtain the acoustic characteristics of the solid airfoil and porous configurations. The integration surface was placed coincident with the airfoil surface. Thus, the predicted acoustic signal is essentially that of thickness and loading noise alone. The noise calculations were started at time t = 0.002 s in order to avoid any additional, "non-physical" noise that may result from relative grid motion, as evidenced by the blip initially seen in the c_l and c_d time histories.

A circular array of 36 equally spaced measuring points, located at a distance of 10 chords from the airfoil center, was used to assess the effects of passive porosity on the acoustic (perturbation) pressure. Acoustic pressures at

four of these points, located at azimuthal angles of $0°$ (TE), $90°$ (suction side), $180°$ (LE), and $270°$ (pressure side), are presented in Figure 7 for the configurations defined in Figure 4. Note that the largest pressure amplitudes occur directly above and below the airfoil, consistent with the dipole nature of the radiated sound. It is in these regions where porosity actually attenuates noise by reducing the amplitude of the largest pressure peaks. Everywhere else, porosity tends to increase high frequency noise (thickness noise). This trend is strongest in the vicinity of the LE, where the changes to the effective aerodynamic shape of the airfoil are more evident (see Figure 7c).
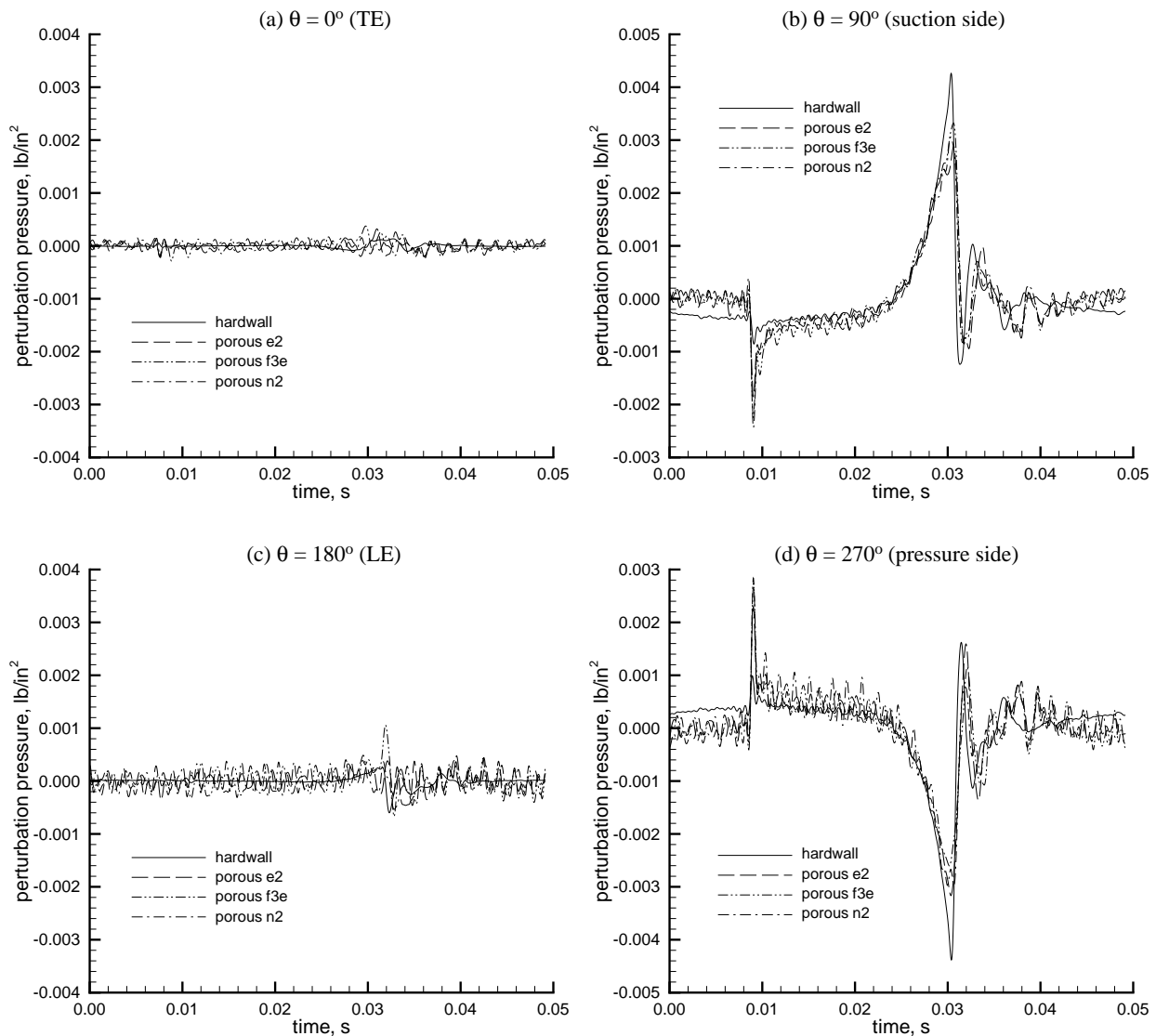

Figure 7.- Perturbation pressure reception time histories for observer at 10 chords from stator surface, fine grid.
$M_\infty = 0.166$, wake $\omega = 78$ c/s.

The effects of passive porosity on radiated wake-stator interaction noise are presented in Figure 8, in terms of overall sound pressure levels (OASPL), for configurations e2, f3e, and n2. The dipole nature of the noise radiated by the airfoils is apparent. A comparison among the solid airfoil and the configurations having continuous porous patches, e2 and f3e, indicates that the noise radiated from the suction side of the airfoil ($0^o < \theta < 180^o$) increases as the extension of the porous patch on the pressure side increases, including noticeable increments in thickness noise ($\theta \sim 0^o$ and $\theta \sim 180^o$). This latter effect is more pronounced for configuration f3e, which has a more extensive porous region on the airfoil pressure side. Although not shown here, it was found that when the porous region on the pressure side extends beyond $x/c \sim 0.2$, the effect of passive porosity is to increase suction side radiated noise above solid airfoil levels. The opposite trend is observed on the pressure side. In general, extending the porous region tends to decrease the noise radiated from this side. This behavior is most likely related to the fact that the rate of pressure venting, which occurs through the plenum from high pressure regions on the pressure side to low pressure regions on the suction side, increases with increasing patch extension.

Also note from Figure 8 that, if the LE region is kept solid (configuration n2), the porous patch on the pressure side of the airfoil can be extended beyond $x/c \sim 0.2$ and still obtain reductions in radiated noise. This effect can be attributed to the fact that, when the region of highest pressure differential, i.e., the LE, is no longer included in the process, the changes in effective LE geometry associated with passive porosity are reduced.

Thus, the presence of porosity reduced peak noise levels by approximately 1.0 dB on both suction and pressure sides for configurations e2 and n2, and by 1.5 dB on the pressure side for configuration f3e.

In order to isolate the effects of porosity on loading noise, which is the main contributor to the noise radiated by the airfoil, sound pressure levels (SPL) were also calculated for the fundamental frequency only. These levels are shown in Figure 9. Although the higher harmonics were found to be important contributors to radiated noise, fundamental frequency noise is dominant, especially for the solid stator. As seen in the figure, peak levels for the solid airfoil are only 5 dB down from the full-spectrum noise levels of Figure 8. From the perspective of loading noise alone, configuration e2 is clearly the better performer, yielding a 2.5 dB noise reduction on both lobes. Configuration n2 is a close second, with an average reduction in peak noise of about 2.0 dB.
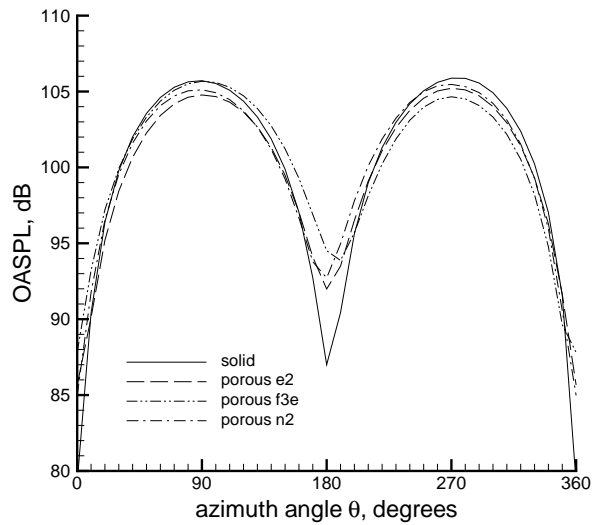

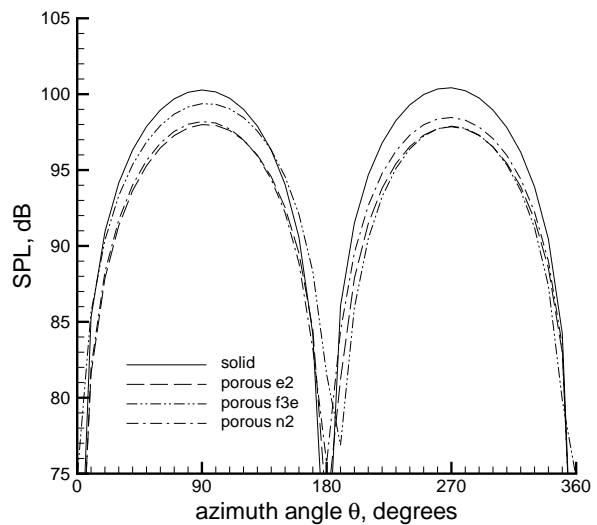Figure 8.- OASPL at 10 chords from source, fine grid.

Figure 9.- SPL at 10 chords from source, fundamental frequency only, fine grid.

Conclusions

The potential of Passive Porosity Technology as a mechanism to reduce wake-stator interaction noise by reducing the unsteady lift developed on the stator surfaces has been evaluated. In order to do so, a typical fan stator airfoil was immersed in a subsonic flow field and subjected to the effects of a transversely moving wake. Solutions were obtained for a solid airfoil baseline, and for a series of porous configurations in order to identify those that would reduce radiated noise without compromising airfoil performance. In general, noise reductions were obtained for those configurations having passive porosity in the LE region of the airfoil between $x/c \sim 0.15$ on

the suction side and x/c ~ 0.20 on the pressure side. Variations in the magnitude of porosity were of secondary importance. The presence of passive porosity reduced loading noise but increased thickness noise. Overall reductions in peak radiated noise of approximately 1 dB were obtained. This reduction increases to about 2.5 dB if only the effects of loading noise are considered.

Acknowledgements

References

1. Kramer, J. J., Hartmann, M. J., Leonard, B. R., Klapproth, J. F., and Sofrin, T. G., "Fan Noise and Performance," Aircraft Engine Noise Reduction, NASA SP-311, May 1972.

2. Dittmar, J. H., "Methods for Reducing Blade Passing Frequency Noise Generated by Rotor-Wake - Stator Interaction," NASA TM X-2669, November 1972.

3. Lowson, M. V., "Reduction of Compressor Noise Radiation," Journal of the Acoustic Society of America, Vol. 43, No. 1, 1968.

4. Majjigi, R. K., and Gliebe, P. R., "Development of a Rotor Wake/Vortex Model," Volume 1 - Final report, NASA CR-174849, June 1984.

5. Horlock, J. H., "Fluctuating Lift Forces on Aerofoils Moving Through Transverse and Chordwise Gusts," Transactions of the ASME, Journal of Basic Engineering, December 1968.

6. Kemp, R. H, Hinchberg, M. H., and Morgan, W.C., "Theoretical and Experimental Analysis of the Reduction of Rotor Blade Vibration in Turbomachinery through the use of Modified Stator Vane Spacing," NACA TN 4373, September 1958.

7. Sharland, I. J., "Sources of Noise in Axial Flow Fans," Journal of Sound and Vibration, vol. 1, 1964.

8. Simonich, J., Lavrich, P., Sofrin, T., and Topol, D., "Active Aerodynamic Control of Wake-Airfoil Interaction Noise - Experiment," DGLR/AIAA 92-02-038, May 1992.

9. Wood, R. M., Banks, D. W., and Bauer, S. X. S., "Assessment of Passive Porosity with Free and Fixed Separation on a Tangent Ogive Forebody," AIAA 92-4494, August 1992.

10. Tinetti, A. F., "On the Use of Surface Porosity to Reduce Wake-Stator Interaction Noise," Ph. D. dissertation, Virginia Polytechnic Institute and State University, September 2001.

11. Frink, N. T., Bonhaus, D. L., Vatsa, V. N., Bauer, S. X. S., and Tinetti, A. F., "A Boundary Condition for Simulation of Flow over Porous Surfaces," AIAA 2001-2412, June 2001.

12. Krist, S. L., Biedron, R. T., and Rumsey, C. L., CFL3D User's Manual, Version 5.0, November 1996.

13. Tinetti, A. F., Kelly, J. J., Bauer, S. X. S., and Thomas, R. H., "On the Use of Surface Porosity to Reduce Unsteady Lift," AIAA 2001-2921, June 2001.

14. Lockard, D. P., "An Efficient, Two-Dimensional Implementation of the Ffowcs-Williams and Hawkings Equation", Journal of Sound and Vibration, 229(4), 2000, pages 897-911.

15. Bush, R. H., "Engine Face and Screen Loss Models for CFD Applications," AIAA 97-2076, June 1997.

16. Menter, F., "Zonal Two Equation k-ω Turbulence Models for Aerodynamic Flows," AIAA 93-2906, 1996.

17. Thomas, R. H., Gerhold, C. H., Farassat, F., Santa Maria, O. L., Nuckols, W. E., and DeVilbiss, D. W., "Far Field Noise of the 12 Inch Advanced Ducted Propeller Simulator," AIAA 95-0722, January 1995.

18. Goldstein, M. E., Aeroacoustics, Chapter 2, NASA SP-346, 1974.

19. Singer, B. A., Brentner, K. S., Lockard, D. P., and Lilley, G. M., "Simulation of Acoustic Scattering from a Trailing Edge", AIAA 99-0231, January 1999.

20. Singer, B. A., Lockard, D. P., Brentner, K. S., Khorrami, M. R., Berkman, M. E., and Choudari, M., "Computational Aeroacoustic Analysis of Slat Trailing-Edge Flow", AIAA 99-1802, May 1999.

21. Bauer, S. X. S., and Hemsch, M. J., "Alleviation of Side Force on Tangent-Ogive Forebodies Using Passive Porosity," AIAA 92-2711, June 1992.

22. Atassi, H. M., Subramaniam, S., and Scott, J. R., "Acoustic Radiation from Lifting Airfoils in Compressible Subsonic Flow," AIAA 90-3911, October 1990.